4274–4284 *Nucleic Acids Research, 2010, Vol. 38, No. 13* *Published online 22 March 2010*
doi:10.1093/nar/gkq174

Quantitative profiling of the full *APOBEC3* mRNA repertoire in lymphocytes and tissues: implications for HIV-1 restriction

Eric W. Refsland, Mark D. Stenglein, Keisuke Shindo, John S. Albin, William L. Brown and Reuben S. Harris*

Department of Biochemistry, Molecular Biology and Biophysics, Institute for Molecular Virology, Center for Genome Engineering, Masonic Cancer Center, University of Minnesota, Minneapolis, MN 55455, USA

Received November 27, 2009; Revised February 28, 2010; Accepted March 2, 2010

ABSTRACT

The human APOBEC3 proteins are DNA cytidine deaminases that impede the replication of many different transposons and viruses. The genes that encode APOBEC3A, APOBEC3B, APOBEC3C, APOBEC3D, APOBEC3F, APOBEC3G and APOBEC3H were generated through relatively recent recombination events. The resulting high degree of inter-relatedness has complicated the development of specific quantitative PCR assays for these genes despite considerable interest in understanding their expression profiles. Here, we describe a set of quantitative PCR assays that specifically measures the mRNA levels of each *APOBEC3* gene. The specificity and sensitivity of each assay was validated using a full matrix of *APOBEC3* cDNA templates. The assays were used to quantify the *APOBEC3* repertoire in multiple human T-cell lines, bulk leukocytes and leukocyte subsets, and 20 different human tissues. The data demonstrate that multiple *APOBEC3* genes are expressed constitutively in most types of cells and tissues, and that distinct *APOBEC3* genes are induced upon T-cell activation and interferon treatment. These data help define the *APOBEC3* repertoire relevant to HIV-1 restriction in T cells, and they suggest a general model in which multiple APOBEC3 proteins function together to provide a constitutive barrier to foreign genetic elements, which can be fortified by transcriptional induction.

INTRODUCTION

The APOBEC3 (A3; apolipoprotein B mRNA-editing enzyme, catalytic polypeptide-like 3) proteins are Zn^{2+}-dependent DNA cytidine deaminases, which are capable of inhibiting the replication of an incredible range of mobile genetic elements (1–4). In humans, representative A3 substrates include exogenous retroviruses such as HIV-1 and HTLV, endogenous retroviruses such as HERV, endogenous retrotransposons such as L1 and Alu, and DNA viruses such as HBV and HPV (5–15). Despite the relevance of many of these parasitic elements to human health, the A3 proteins that function *in vivo* against each particular element have yet to be defined. For instance, A3F and A3G have been shown to strongly restrict HIV-1 *in vitro* and very likely contribute to HIV-1 restriction *in vivo*, but strong arguments have also implicated several other human A3 proteins (1–4,16).

The seven *A3* genes are positioned in tandem on human chromosome 22: *A3A*, *A3B*, *A3C*, *A3D* (formerly *A3DE*), *A3F*, *A3G* and *A3H* (17). A defining feature of each *A3* gene is that it encodes a protein with one or two conserved zinc (Z)-coordinating deaminase domains. Each Z domain belongs to one of three distinct phylogenetic groups: Z1 (A3A and the C-terminal halves of A3B and A3G), Z2 (A3C, both halves of A3D and A3F, and the N-terminal halves of A3B and A3G) and Z3 (A3H) (18). Based on the relatedness of these Z domains, the human *A3* repertoire appears to be the result of a minimum of eight unequal

*To whom correspondence should be addressed. Tel: +1 612 624 0457; Fax: +1 612 625 2163; Email: rsh@umn.edu
Present address:
Mark D. Stenglein, Departments of Medicine, Biochemistry and Microbiology, Howard Hughes Medical Institute, University of California, San Francisco, CA 94143, USA.

The authors wish it to be known that, in their opinion, the first two authors should be regarded as joint First Authors.

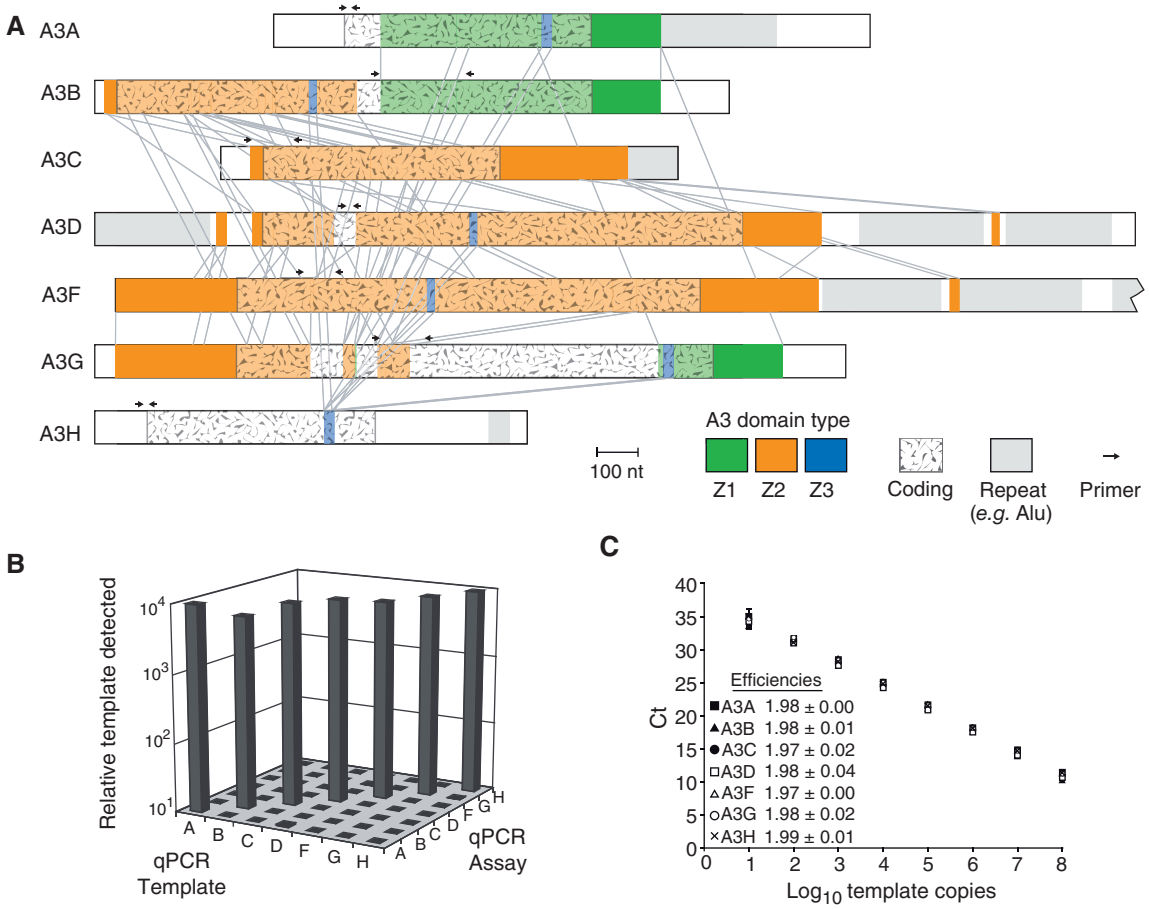

Figure 1. A panel of quantitative PCR assays to monitor *APOBEC3* mRNA levels. (**A**) Overview of *A3* mRNA features. Each *A3* mRNA is depicted to scale except 2100 nt of the *A3F* 3′ UTR are not shown. Inter-*A3* regions of 90% or greater identity over ≥18 nt are highlighted in color. (**B**) A histogram depicting the results of running each *A3* qPCR assay against each of the seven *A3* cDNA control templates. (**C**) A graph showing the *A3* qPCR assay amplification ranges and efficiencies. The mean and standard deviation of two independent experiments each consisting of three replica reactions is shown (in most instances the error is smaller than the symbol).

crossing-over recombination events, which mostly occurred during the radiation of primates (18). The net result is that the human *A3* mRNAs share considerable identity, ranging from 30% to nearly 100% (Figure 1A and Supplementary Table S1). For example, nt 1–473 of the *A3F* mRNA are 98.7% identical to *A3G* nt 50–522. Similarly, *A3A* nt 259–937 are 96.6% identical to the corresponding region of *A3B*, nt 692–1370. The *A3* genes are also under positive selection and accordingly are highly polymorphic (19–21). These inter-domain identities and polymorphisms present considerable challenges to *A3* expression profiling and quantification.

Here we report specific quantitative PCR (qPCR) assays for each of the seven human *A3* cDNA sequences. We use these assays to profile the expressed *A3* repertoire in common T-cell lines, primary $CD4^+$ T lymphocytes, and 20 distinct human tissues. We also quantify the effects of T-cell stimulation and interferon (IFN) induction on *A3* expression. These expression data indicate that several A3 proteins, in addition to A3F and A3G, are expressed in $CD4^+$ cells and are therefore positioned to contribute to HIV-1 restriction. More generally, nearly every cell type and tissue expresses multiple *A3*s, consistent with a model in which parasitic elements must evolve ways to cope with a constitutive set of restriction factors that can be further fortified by transcriptional induction.

MATERIALS AND METHODS

Cell lines

Human T-cell lines were cultured in RPMI (ThermoFisher) supplemented with 10% fetal bovine serum (Denville). SupT1 and H9 were obtained from the AIDS Research and Reference Reagent Program. SupT11 is a sub-clone of SupT1 obtained by limiting dilution. CEM and CEM-SS were described (22).

Enrichment and culture of primary cells

Peripheral blood mononuclear cells (PBMCs) were isolated from blood (Memorial Blood Center, St. Paul, MN) by Ficoll-Paque gradient centrifugation (GE Healthcare). The resulting buffy coat was subjected to negative selection to enrich for naïve primary $CD4^+$ T cells (Miltenyi Biotech). Primary cells were cultured in RPMI supplemented with 10% FBS and stimulated to proliferate with 50 U ml^{-1} recombinant interleukin-2 (IL-2; Sigma), and 10 μg ml^{-1} phytohemagglutinin

Table 1. *APOBEC3* qPCR primers and probes

Gene symbol	mRNA NCBI accession	5′ Primer Name	Seq (5′–3′)	3′ Primer name	Seq (5′–3′)	Probe name	Seq[a]
APOBEC3s							
APOBEC3A	NM_145699	RSH2742	gagaagggacaagcacatgg	RSH2743	tggatccatcaagtgtctgg	UPL26	ctgggctg
APOBEC3B	NM_004900	RSH3220	gacccttggtccttcgac	RSH3221	gcacagccccaggagaag	UPL1	cctggagc
APOBEC3C	NM_014508	RSH3085	agcgcttcagaaaagagtgg	RSH3086	aagtttcgttccgatcgttg	UPL155	ttgccttc
APOBEC3D	NM_152426	RSH2749	acccaaacgtcagtcgaatc	RSH2750	cacatttctgcgtggttctc	UPL51	ggcaggag
APOBEC3F	NM_145298	RSH2751	ccgtttggacgcaaagat	RSH2752	ccaggtgatctggaaacactt	UPL27	gctgcctg
APOBEC3G	NM_021822	RSH2753	ccgaggacccgaaggttac	RSH2754	tccaacagtgctgaaattcg	UPL79	ccaggagg
APOBEC3H	NM_181773	RSH2757	agctgtggccagaagcac	RSH2758	cggaatgtttcggctgtt	UPL21	tggctctg
Reference genes							
TBP	NM_003194	RSH3231	cccatgactcccatgacc	RSH3232	tttacaaccaagattcactgtgg	UPL51	ggcaggag
RPL13A	NM_012423	RSH3227	ctggaccgtctcaaggtgtt	RSH3228	gccccagataggcaaacttt	UPL74	ctgctgcc
HPRT1	NM_000194	RSH2959	tgaccttgatttattttgcatacc	RSH2960	cgagcaagacgttcagtcct	UPL73	gctgagga

[a]It is not known whether the UPL probes correspond to the coding or template DNA strands of their target sequences (Roche proprietary information).

(PHA; Fisher Healthcare). To confirm proliferation, 10^6 cells were stained with 10 μM carboxyfluorescein diacetate succinimidyl ester (CFSE) according to the manufacturer (Invitrogen) and analyzed by flow cytometry. PBMCs and $CD4^+$ T cells were treated with 2 ng ml^{-1} universal type I IFN (R&D Systems).

RNA preparation

PBS-washed cells were prepared for RNA isolation by lysis in ice-cold buffer RLT (Roche) supplemented with 10 μl ml^{-1} 2-mercaptoethanol (Sigma). RNA was isolated using the RNeasy kit (Qiagen). Two optional components of the kit, QiaShredder and on-column DNase digestion, were used to homogenize lysates and remove genomic DNA. RNA concentrations were determined spectroscopically and RNA quality was assessed by gel analysis (Supplementary Figure S1). Total RNA from 20 distinct tissues, each from a minimum of three donors, was purchased from Ambion. The control qPCRs for housekeeping genes (below) were similarly efficient for all RNA preparations, indicating equally high qualities and integrities.

cDNA synthesis

Total RNA (1 μg) was used to synthesize cDNA using avian myeloblastosis virus reverse transcriptase (AMV RT; Roche) and random hexameric primers. We found that random hexamer mRNA priming was preferable to oligo-dT priming, which resulted in inefficient synthesis of some *A3* cDNAs, particularly *A3D* and *A3F*, most likely because of their long, repeat-rich 3′ untranslated regions (UTRs) (Figure 1A and Supplementary Figure S2). cDNA synthesis reactions were performed by mixing 3 μl of 333 μM random hexamer primer (50 μM final concentration) with 1 μg of total RNA diluted in 10 μl of RNase-free water. This mixture was heated for 10 min at 65°C to remove RNA secondary structure and then cooled briefly on ice. Master mix (7 μl) containing 0.5 μl Protector RNase inhibitor (Roche), 0.4 μl AMV RT, 4 μl 5× AMV RT reaction buffer, and 2.1 μl dNTPs (Roche, 10 mM each; ~1 mM each final concentration) were then added to these reactions, which were subsequently incubated at 25°C for 10 min, 42°C for 1 h, then 95°C for 5 min. Reactions were then diluted by addition of 80 μl RNase-free H_2O, and used in qPCR reactions.

qPCR

cDNAs levels were quantified by PCR using a Roche Lightcycler 480 instrument according to the manufacturer's protocols. Reactions were performed in 96-well plates with each containing 7.5 μl 2× probe master mix (Roche), 1.25 μl H_2O, 1.05 μl primers (5 μm each), 0.2 μl UPL probe (Roche) and 5 μl cDNA (prepared as above). Reactions were incubated at 95°C for 10 min, then 40 cycles of 95°C for 10 s, 58°C for 15 s, then 72°C for 2 s. Table 1 lists the full sequences of all primers and probes used in this study; the design rationale and validation experiments are described below. The PCR cycle at which amplification was detectable above a background threshold (threshold cycle, or C_t) was calculated with the maximum second derivative method using the Lightcycler 480 software (Roche, version 1.5.0). cDNA was synthesized and qPCR performed in triplicate for each sample, and the mean values and standard deviations for each triplicate are reported.

Primer design

Primer pairs were designed to avoid inter-*A3* identity and only amplify the intended *A3* target (Figure 1A, Supplementary Figure S2, Table 1 and Supplementary Table S1). Primer pair specificity was verified by manually inspecting alignments of primers and *A3* cDNA sequences, by using BLAST (version 2.2.20; http://blast.ncbi.nlm.nih.gov/) and Primer-BLAST software (http://www.ncbi.nlm.nih.gov/tools/primer-blast/; default parameters except *E* set to 1) and, experimentally, by attempting to amplify 10^4 copies of every *A3* control template with each set of *A3* qPCR primers (Figure 1B). Primers were additionally designed to have similar melting temperatures and were confirmed to have similar reaction efficiencies (Figure 1C and see below). Furthermore, primers were designed such that they

would amplify all described variants of each *A3* mRNA (i.e. splice variants and SNPs; data not shown). Design was assisted by the Roche ProbeFinder software (version 2.43; http://qpcr.probefinder.com/roche3.html) and by Primer3 software (version 0.4.0; http://primer3.sourceforge.net/).

Data analysis

Expression level normalization. *A3* expression data were normalized to the expression of TATA-box binding protein (*TBP*; see below). Essentially identical normalized results were obtained using *ribosomal protein L13A* (*RPL13A*), or *hypoxanthine-guanine phosphoribosyltransferase* (*HPRT*) (data not shown). None of these controls showed altered expression levels upon treatment of cells with IL-2, PMA and/or IFN.

Determination of reaction efficiencies. For all assays, the primer efficiency was determined using serial dilutions of control templates (e.g. Figure 1C). The control templates consisted of portions of the 5′ UTRs and coding regions of the *A3* cDNAs amplified by PCR and cloned into pCR2.1-TOPO (Invitrogen). The same templates were used to validate assay specificity (Figure 1B). These plasmids were linearized by digestion with XmnI or BglII, phenol–chloroform extracted, ethanol precipitated, and the DNA concentration was determined spectroscopically. Ten-fold serial dilutions of these plasmids were prepared with 10^1–10^8 plasmid molecules per 5 µl. These dilutions were used as templates in qPCR reactions. C_t values were plotted against the $\log_{10}$ number of template molecules in each reaction (Figure 1C), and the slope of this line determines the reaction efficiency according to the equation: efficiency $= 10^{(-1/\text{slope})}$ (23). Reaction efficiencies were also calculated from the actual amplification curves from several experiments (24). Reaction efficiencies calculated by these two methods agreed closely (data not shown).

The reaction efficiencies (E) determined in this manner were then used to calculate relative expression levels between two samples (S1 and S2), normalized to a reference gene (ref, *TBP*), according to published methods (23):

$$\Delta Ct_{(A3)} = Ct_{A3,S1} - Ct_{A3,S2}$$
$$\Delta Ct_{(ref)} = Ct_{ref,S1} - Ct_{ref,S2}$$
$$\text{Relative expression} = (E_{A3})^{-\Delta Ct(A3)}/(E_{ref})^{-\Delta Ct(ref)}$$

Immunoblotting

Cells were cultured and/or isolated as described above, washed in PBS and lysed in 0.2% NP40 buffer with 1 × EDTA-free protease inhibitor mixture (Roche). Proteins were subjected to ice-cold acetone precipitation prior to quantification (Bio-Rad). An equal amount of protein was fractionated on a 10% SDS-polyacrylamide gel and transferred to a PVDF membrane (Millipore). Membranes were blotted with antibodies specific to A3F, A3G or tubulin (Covance). The A3F and A3G polyclonal antibodies were obtained from the AIDS Research and Reference Reagent Program courtesy of M. Malim (Kings College London) and J. Lingappa (University of Washington), respectively (25,26). Band intensities were quantified using Image J software (NIH).

RESULTS

APOBEC3 qPCR assay designs and optimization experiments

To determine where and when each *A3* mRNA is expressed we developed a panel of specific qPCR assays. For each assay, several computational and manual procedures were used to develop specific and efficient qPCR primers. Each primer was selected to span two exons (Figure 1A and Table 1). The primers and probes were screened to avoid known single nucleotide polymorphisms and splice variations (data not shown). Assay specificity was tested by pitting all seven qPCR probe/primer sets against each of the seven *A3* cDNA templates in a 49-reaction qPCR matrix. The amplification results demonstrated that each assay was specific to the intended target *A3* (Figure 1B).

The next most important parameter to test and optimize was reaction efficiency. Serial dilutions of linearized *A3* control cDNA templates were used in qPCR reactions to measure efficiencies. After as many as four primer/probe redesigns for some *A3*s, high efficiencies ranging from 1.97–1.99 were achieved for each qPCR assay (Figure 1C). These nearly ideal efficiencies indicated that each assay would provide a robust and quantitative measure of the level of expression of each *A3* gene. In other words, these data indicated that quantitative comparisons of each *A3* relative to the others are possible.

Assay standardization and normalization are crucial parameters to ensure quantitative data set comparisons. We therefore also designed and tested qPCR assays for three common housekeeping genes, *TBP*, *RPL13A* and *HPRT* ('Materials and Methods' section). The mRNA levels of each of these genes were consistent between cell types and tissues. To facilitate data normalization and comparisons, only one of these genes (*TBP*) was used as an internal standard.

Finally, each of the aforementioned *A3* qPCR assays was evaluated on two independent platforms to ensure that all data could be reproduced and generalized. The Roche Lightcycler 480 platform, which uses fluorescent probes, was used to develop the assays and for all data reported here. A similar set of reaction specificities was observed using different instrumentation and detection methods (iCycler and SybrGreen, respectively; BioRad, data not shown). These data indicated that our *A3* qPCR assays could be applied to a range of experimental questions.

APOBEC3 expression profiles in permissive and non-permissive T-cell lines

Three groups independently discovered A3G in 2002 (5,17,27). One of these studies was based on the observation that there are two distinct phenotypes in human T-cell lines with respect to Vif-deficient HIV-1 infection (5,28–30). Cell lines such as CEM and H9 are resistant to infection by Vif-deficient viruses and, accordingly, are

termed non-permissive. On the other hand, cell lines such as CEM-SS (a clonal derivative of CEM) and SupT1 support HIV-1 replication in the presence or absence of Vif and are thus deemed permissive. A3G was originally identified as the dominant restriction factor whose presence accounted for the non-permissive phenotype of CEM cells in comparison to its permissive daughter line, CEM-SS. Since then, overexpression of several A3 family members has been shown to render CEM-SS non-permissive to Vif-deficient HIV replication (1–5,16,22). Despite the elegance of this permissive and non-permissive dichotomy, the full nature of the Vif-deficient HIV-1 replication defect on non-permissive cells has not been elucidated. In other words, which A3s are required for HIV-1 restriction in non-permissive cells: A3G or some combination of A3G and these other A3 proteins?

To shed additional light on this important question, we profiled the expressed *A3* repertoire in the two related cell lines, non-permissive CEM and permissive CEM-SS. These cell lines were used to clone *A3G* by subtractive hybridization (5) and, as expected, *A3G* mRNA levels were 12-fold higher in the non-permissive line CEM (Figure 2A). However, levels of *A3B*, *A3C*, *A3D* and *A3F* were also significantly higher than those in CEM-SS, by 19-, 2-, 3- and 28-fold, respectively. These observations suggest that other A3s, in addition to A3G, may contribute to Vif-deficient HIV-1 restriction in CEM. However, the presence of significant *A3C* mRNA levels in CEM-SS is concordant with it alone not being sufficient to restrict the replication of Vif-deficient HIV-1 (31,32).

Further consistent with the possibility that multiple A3s contribute to the non-permissive phenotype, the non-permissive T-cell line H9 was also found to express multiple *A3* mRNAs at levels well beyond those in permissive cells (Figure 2B). *A3C*, *A3D*, *A3F*, *A3G*, and *A3H* were 2-, 8-, 16-, 19- and 1000-fold above those in CEM-SS cells, respectively. In contrast to CEM cells, *A3B* was virtually absent, and *A3H* was well expressed (considered further below). Notably, the expression levels of all seven *A3* genes were extremely low and approaching detection limits in the permissive line SupT11. Thus far, SupT11 is the only T-cell line that we have found that is practically devoid of *A3* gene expression. The molecular explanation for this is not known, but it is not due to deletion of the locus because specific qPCR products are still detected.

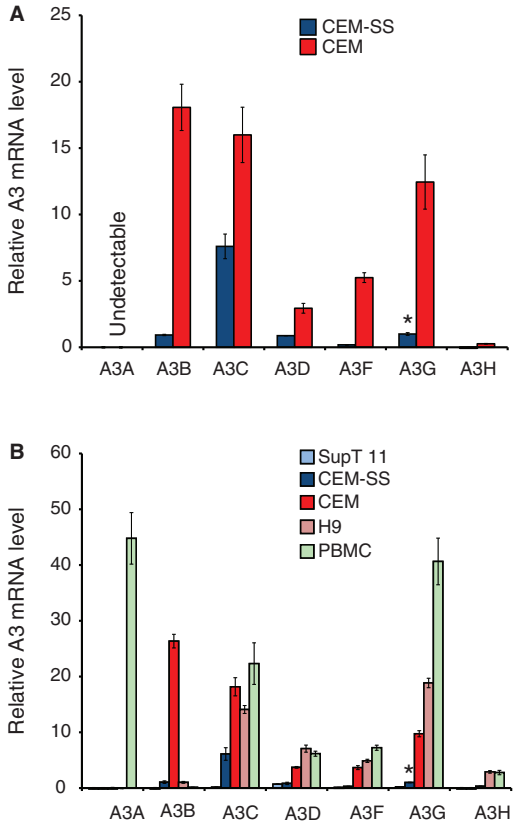

Figure 2. *APOBEC3* expression in human T-cell lines and naïve PBMCs. (**A**) *A3* expression in the permissive T-cell line CEM-SS and the non-permissive line CEM. Mean values and standard deviations of three independent qPCR reactions are shown for each condition. Expression is normalized to the reference gene *TBP* and the level of CEM-SS *A3G* is set to 1 to facilitate comparison (denoted by the asterisk). (**B**) *A3* expression in the permissive T-cell lines SupT11 and CEM-SS in comparison to non-permissive lines CEM and H9. The expressed *A3* repertoire in PBMCs is shown for comparison (data from an independent experiment in which CEM and CEM-SS yielded results similar to those shown here). The experimental parameters are identical to those used in panel A.

APOBEC3 expression profiles in primary leukocytes

Next we sought to define the *A3* repertoire in fresh, unstimulated PBMCs (Figure 2B). Multiple *A3*s were expressed in PBMCs with the overall pattern resembling that of CEM and H9 non-permissive lines (significant levels of *A3C*, *A3D*, *A3F* and *A3G*). However, some major differences were detected. First and most strikingly, PBMCs were found to express high *A3A* levels, which were ~5000-fold greater than CEM. These observations were consistent with recent reports indicating that *A3A* expression is specific to the $CD14^+$ lineage, which includes macrophages and monocytes (11,33–35). Second, PBMCs expressed virtually no *A3B* mRNA, which is ~100-fold less than CEM. Third, PBMCs expressed 4-fold more A3G than CEM, and 40-fold more than CEM-SS. Finally, PBMCs were found to express high levels of A3H, similar to those observed in H9, ~13-fold more than CEM, and nearly 1000-fold more than CEM-SS or SupT11.

The expressed *APOBEC3* repertoire in naïve and stimulated $CD4^+$ T lymphocytes

$CD4^+$ T lymphocytes are a major target of HIV-1. To define the expressed *A3* repertoire in this important T-cell subset, we used negative selection to isolate $CD4^+$ lymphocytes from fresh PBMCs (Figure 3A). These cells were stimulated with IL-2 and PHA and shown to proliferate by CFSE staining and flow cytometry (Figure 3B). T-cell stimulation caused the induction of every *A3* with the exception of *A3A* (Figure 3C). Mitogen activation had been shown previously to induce A3G expression in $CD4^+$

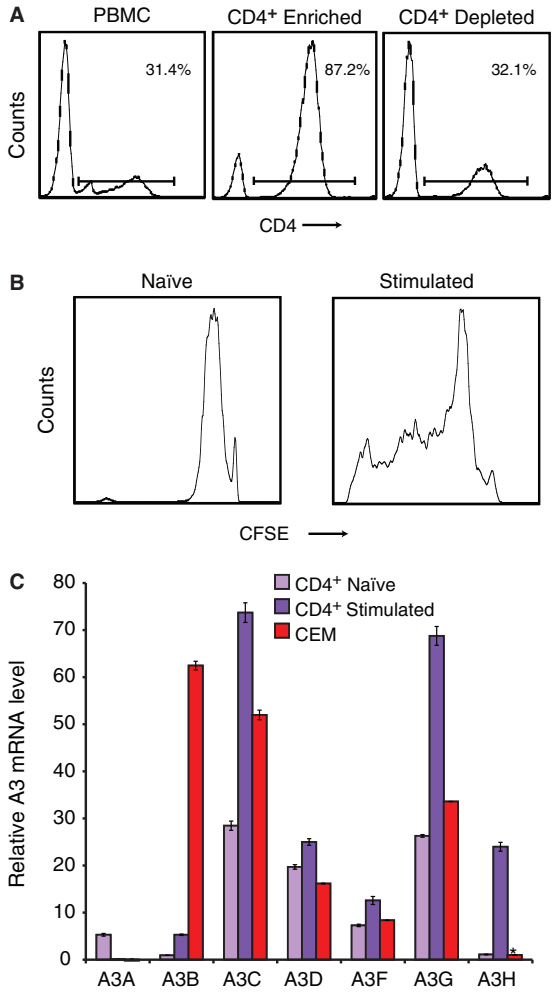

Figure 3. *APOBEC3* expression in naïve and stimulated $CD4^+$ lymphocytes. (**A**) Flow cytometry histograms depicting the results of $CD4^+$ lymphocyte purification by negative selection. (**B**) Flow cytometry histograms of CFSE-labeled cells 4 days after mock or IL-2/PHA treatment, naïve and stimulated, respectively. (**C**) *A3* expression in naïve and 3 day stimulated $CD4^+$ lymphocytes. Data from CEM are shown for comparison. Expression is normalized to *TBP* and the level of *A3H* in CEM is set to 1 (denoted by the asterisk). Mean values and standard deviations of three independent qPCR reactions are shown for each condition.

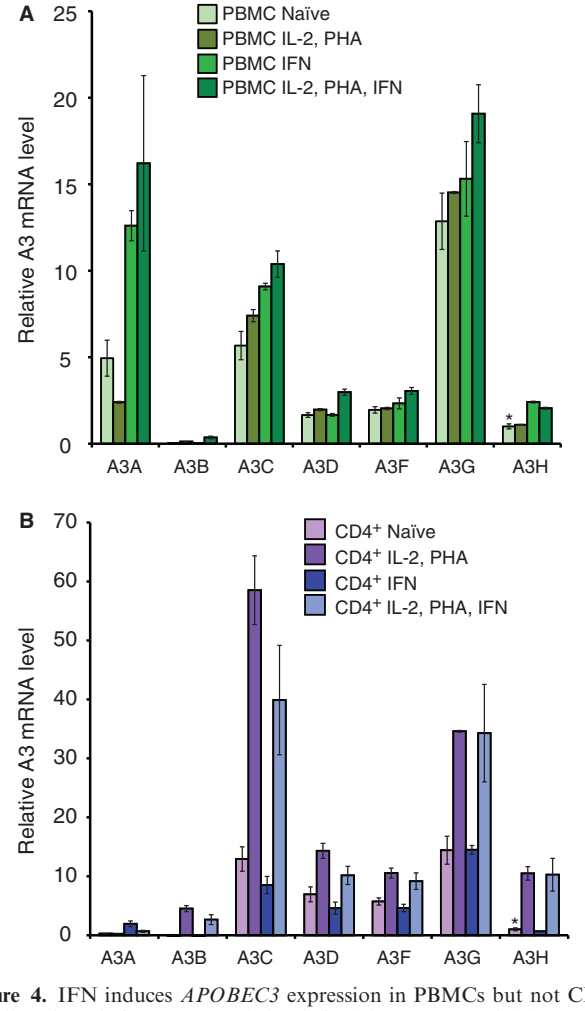

Figure 4. IFN induces *APOBEC3* expression in PBMCs but not $CD4^+$ T cells. The relative *A3* mRNA levels in (**A**) PBMCs and (**B**) $CD4^+$ T lymphocytes treated for 48 h with IL-2/PHA and/or IFN. Expression is normalized to *TBP* and the naïve *A3H* level is set to 1 (denoted by the asterisk). Mean values and standard deviations of three independent qPCR reactions are shown for each condition.

T cells (35,36). The increase in *A3H* expression levels is particularly remarkable, rising 22-fold over naïve levels.

Several *APOBEC3*s are IFN-responsive

In response to viral infection, cytokines such as type I IFNs are induced, and these in turn activate the expression of hundreds of genes. Several *A3*s have been shown to be IFN-responsive, but only two reports have considered the entire *A3* repertoire and procedures have varied considerably [(11,35,37–43); see 'Discussion' section]. To extend this work, fresh PBMCs were treated with leukocyte IFN and the resulting *A3* mRNA levels were quantified by qPCR (Figure 4A). In bulk PBMCs, *A3A* was clearly induced, in agreement with prior reports (11,35,40,44). The other *A3*s were also found to be up-regulated but to lesser extents.

We next examined the effects of IL-2, PHA and IFN on *A3* expression in naïve and stimulated $CD4^+$ T cells (Figure 4B). As shown above, the T-cell mitogens IL-2 and PHA induced the mRNA levels of all of the *A3*s except *A3A* (compare Figures 3C and 4B). In contrast, IFN treatment did little to alter these expression profiles. Thus, the *A3*s in $CD4^+$ T lymphocytes are not IFN inducible, whereas the *A3*s in at least one other PBMC cell type are IFN-responsive. Based on recent reports, $CD14^+$ phagocytic cells such as monocytes and macrophages are likely to be the only leukocyte subset in which *A3* expression is IFN-inducible [(11,35,40,44) and data not shown].

APOBEC3 expression profile in human tissues

An important question with respect to *A3* expression is whether or not it is confined to immune cell compartments. To help address this issue, we quantified the expressed *A3* repertoire of twenty normal human tissues. Two cell lines, CEM and SupT11, and fresh PBMCs were assayed in parallel to facilitate comparisons with

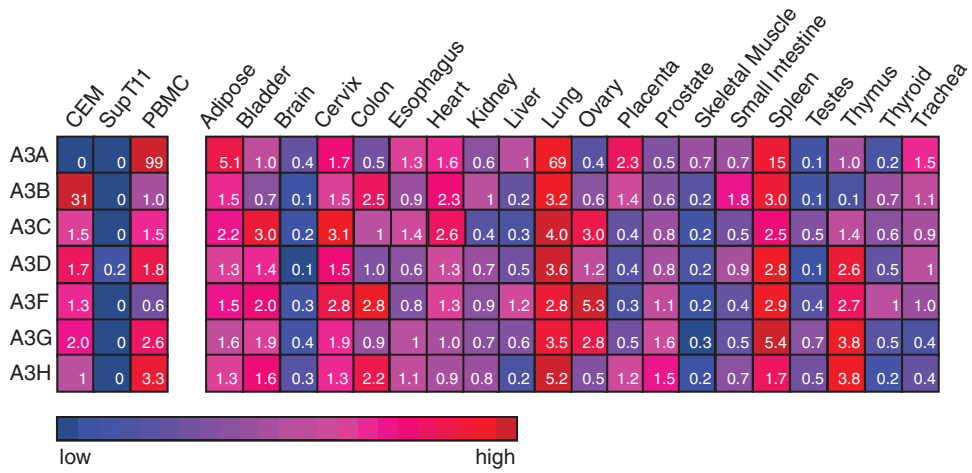

Figure 5. *APOBEC3* expression in human tissues. A summary of qPCR data showing the relative *A3* mRNA levels in the indicated cells and tissues. The color scheme provides qualitative information, as the full range of blue (low expression) to red (high expression) color is used for each row of data. The inset numbers represent the relative levels of each *A3* mRNA across the panel with the median value in each row set to 1. Since the assay efficiencies are almost identical (Figure 1C), these quantitative data can be used to compare any of the values within the table. Three replicas were done for each condition and the average values were used to construct the table (the errors were <10% and are not shown for simplicity).

our other data sets. Several interesting observations emerged from these studies (Figure 5).

First, consistent with central roles in innate immunity, *A3* expression levels were high in lymphoid organs such as the thymus and spleen. The thymus, which is rich in T lymphocytes, has an expressed *A3* repertoire similar to that of primary $CD4^+$ T cells: low *A3A* and *A3B*, high *A3C*, *A3D*, *A3F*, *A3G* and *A3H* (compare Figures 5 and 3C). The spleen is rich in both B and T lymphocytes, but it is also a major reservoir for undifferentiated monocytes (45). This helped reconcile observations showing that the spleen has relatively high levels of all seven *A3*s, consistent with previous observations indicating that *A3A* is restricted to $CD14^+$ cells including monocytes (11,35,40).

Second, many *A3*s were clearly expressed outside of the blood compartment or common immune tissues. For example, five of seven *A3*s showed peak expression levels in lung tissue: *A3A*, *A3B*, *A3C*, *A3D* and *A3H*. The most remarkable was *A3A*, which was detected at levels 70-fold higher in the lung than the median value from all 20 tissues. This observation is consistent with large numbers of $CD14^+$ macrophages residing in lung alveoli. A bronchoalveolar lavage cell preparation from a non-smoking individual yields 1×10^7 cells, of which 90–95% are macrophages (46). In addition, *A3A* was expressed in adipose tissue at levels 5-fold higher than the median value. This level is compatible with the finding that adipose from an obese individual is 40% macrophages by weight (47). Also of note is *A3* expression in the ovary. Levels of *A3C*, *A3F* and *A3G* were 3-, 5- and nearly 3-fold higher, respectively, than median values from the other tissues. This may indicate a requirement for viral and transposable element restriction in female germ cells (48).

Finally, some tissues expressed virtually no *A3*s. The brain and the testes, for instance, had low *A3* levels comparable to those of SupT11 (compare Figures 5 and 2B). These are largely immune privileged organs that are physically separated from other tissues and from potential pathogen infections by the blood–brain barrier and the blood–tubular barrier, respectively. The apparent *A3* expression deficiency in these tissues may also be due in part to the absence of appropriate gene expression activators such as IFNs, cytokines and/or growth factors.

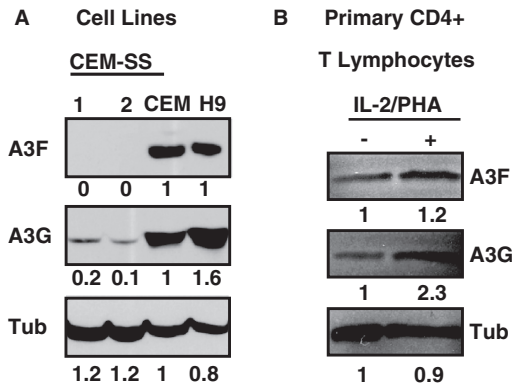

Figure 6. APOBEC3 immunoblots. (**A**) T-cell line or (**B**) primary $CD4^+$ lymphocyte (IL-2/PHA or mock treated) protein extracts were examined by immunoblotting with antibodies specific to A3F or A3G.

Strong correlations between *APOBEC3* mRNA and protein expression levels

To ask whether the observed *APOBEC3* mRNA levels correlate with protein levels, we separated cell extracts by SDS–PAGE and probed the resulting blots with antibodies raised against A3F and A3G (Figure 6). The A3F polyclonal antibody is specific to the best of our knowledge [(22,25) and unpublished observations]. The A3G polyclonal antibody is semi-specific as it reacts with both A3A and A3G, but these proteins are distinguishable by size (11,26,35).

In strong agreement with our qPCR data and many prior studies, A3F and A3G protein levels are considerably lower in CEM-SS than they are in the non-permissive lines CEM [e.g. Figure 6A; (22,49)]. The low but still measurable levels of A3G in the CEM-SS population also enabled quantification by densitometry, revealing a 5–10-fold difference at the protein level between these two lines. This value closely resembles the 10-fold difference in *A3G* mRNA levels between CEM and CEM-SS (Figure 2). In further agreement with our qPCR data, A3G protein was too low to detect by immunoblotting in SupT11 and ~1.6-fold higher in H9 than CEM. As for A3F, nearly equivalent protein levels were observed in H9 and CEM, and it was undetectable in SupT11 and CEM-SS (Figures 2 and 6A). Finally, we compared the protein expression of A3F and A3G in primary $CD4^+$ T lymphocytes under naïve and stimulated conditions. Consistent with our qPCR data, A3F was induced slightly and A3G levels increased ~2-fold upon T-cell stimulation (Figures 3C and 6B). Overall, we conclude that strong correlations are evident between the qPCR results and the immunoblot data.

DISCUSSION

Despite remarkable progress identifying A3 restriction substrates such as HIV-1, transposons, and foreign DNA, the overarching biological functions of the A3 repertoire are still being elucidated (1–5,11,50). What events drove the rapid expansion of the *A3* locus to encode seven A3 proteins, and a total of eleven zinc-coordinating domains? Does each A3 protein serve some unique, divergent function or do they serve the same function only in different places and/or at different times? How much redundancy exists? How much specificity? How much of this is governed by transcriptional programs? To begin to address the latter question, in particular, here we report qPCR assays that enable the specific and quantitative detection of the entire seven gene human *A3* repertoire. We have improved on previous commercial methods by reporting the identity, specificity and efficiency of each *A3* primer/probe set, by demonstrating the assay's functionality and usefulness across detection platforms and, most importantly, by quantifying *A3* expression in multiple human tissues and cell types. During the course of completing our experiments, an independent study on *A3* expression in hematopoietic cells and tissues was published by Koning *et al.* (35). These two studies are largely complementary, but some differences merit discussion.

The first point is technical. We developed our own qPCR assays and, as such, were able to ensure target specificity and near identical reaction efficiencies (Figure 1). We also report the nucleotide sequences of the primers and probes so the assays are fully compatible with many different qPCR methods and instruments (Table 1). In contrast, Koning *et al.* used proprietary primers and probes from Applied Biosystems, which are optimized for specific reagents and instrumentation and less readily adaptable to other platforms. Knowledge of the primer binding sites is also crucial for detecting and ultimately ascertaining the function of alternatively spliced *A3* variants.

Second, our study uniquely focuses on the question of which A3s are expressed in such a manner that they may contribute to HIV-1 restriction *in vivo*. The observation that the non-permissive T-cell lines CEM and H9 express significantly higher levels of *A3G* and *A3F* is not surprising (Figure 2). However, what is notable is that six *A3*s (i.e. all but *A3A*) are expressed at higher levels in these non-permissive cell lines. The constitutive *A3* repertoire in H9 appears remarkably similar to the induced repertoire in stimulated, primary $CD4^+$ T lymphocytes (Figures 2B and 3C). *A3H* levels, in particular, increase over 20-fold upon T-cell stimulation with IL-2 and PHA. Together with prior cell culture overexpression studies indicating that A3H can restrict HIV-1 in a Vif susceptible manner (20,51–55), our expression data strengthen the case that A3H may contribute to HIV-1 restriction *in vivo*. In contrast, a role for A3A in HIV-1 restriction in $CD4^+$ T cells is unlikely, because it is not expressed in this cell type and it does not restrict Vif-deficient HIV-1 in overexpression experiments [this study and (11,31,33,35)]. Unambiguously testing the involvement of other A3s in HIV-1 restriction, in addition to A3F and A3G, will require much further work.

Third, based on an extensive survey of *A3* expression in 20 tissues, we conclude that the *A3* mRNAs are expressed broadly and not confined to cells of the immune compartment (although there is clearly some bias to immune cell types; Figure 5). For example, adipose, colon, cervix, bladder and the heart all express at least two *A3*s at levels 2-fold above the median among all tissues. In partial contrast, Koning *et al.* concluded that, apart from germ cell tissues, *A3* expression is confined to the hematopoietic compartment and that their detection in many tissues is simply due to infiltrating leukocytes (35). This is likely the case for some tissues such as lung and adipose where significant numbers of *A3A*-expressing macrophages are found. Although the true breadth of *A3* expression in human tissues (and a different developmental stages) will not be fully appreciated until suitably specific immunohistochemistry antibodies are developed, at least two additional lines of evidence support the likelihood that *A3*s are expressed broadly. First, as noted by Koning *et al.* and as is also evident in our data sets, the *A3G* mRNA levels typically exceed those of *A3F* in PBMCs and in specific leukocyte types [Figures 3C, 4 and 5; (35)]. This ratio is inverted in some tissues such as the cervix, colon and ovary, strongly suggesting that immune cell infiltration is not the whole story [Figure 5 and (35)]. Second, many clonally derived cancer cell lines of non-immune cell origins have been shown to express multiple human A3s, such as colorectal hepatocarcinoma, adenocarcinoma, melanoma and lung carcinoma lines [(17,27,38,56–59) and http://www.oncomine.org]. It is possible that *A3* expression switches on at some stage during oncogenesis, but given the abundance of *A3*s in cancer cell lines it is likely that part of this reflects the normal gene expression program that existed prior to immortalization. Thus, the broad and apparently constitutive *A3* expression profile of many human tissues is

consistent with a general role for A3 proteins in innate immunity. Substrates may not only include endogenous and exogenous retroelements, but also DNA viruses and even naked, foreign double-stranded DNA (10–12,60).

Fourth, our data and those of Koning *et al.* (35) are somewhat discordant on the relative difference between *A3G* and *A3F* expression levels. They concluded that the A3G mRNA levels are 10-fold higher than those of A3F. In contrast, we did not observe such a large expression bias. In some tissues such as lung we observed a modest bias in favor of *A3G*. Conversely, in other tissues such as the colon and ovary, we observed a slight bias toward *A3F*. However, in general, we observed that *A3F* and *A3G* levels are fairly similar and that these mRNAs are invariably expressed together. Our data are consistent with prior *A3F* and *A3G* multi-tissue northern blot results and the fact that the promoter regions of *A3F* and *A3G* are 96% identical over a 5-kb region including exons 1 and 2 (56). We favor a model in which A3F and A3G are coordinately expressed [proposed originally by ref. (56)]. A greater understanding of the promoters and their associated transcription factors will help provide future tests of this model. It is possible that differences between the results reported here and the literature are due to protocol differences such as random primed versus oligo-dT mediated cDNA synthesis, the latter being much less efficient and susceptible to repetitive elements in 3′ UTRs, and/or to imperfect PCR reaction efficiencies (e.g. Supplementary Figure S2).

On a strong complementary note, a major point detailed here and in the study by Koning and coworkers is the inducibility of *A3* mRNA expression. Several prior studies have examined the IFN-responsiveness of the *A3*s and particularly *A3G* and the conclusions have been variable (11,35,37–42). However, in agreement with Koning and coworkers, our data indicate that none of the *A3*s are induced by IFN in primary $CD4^+$ T lymphocytes (Figure 4B). Small increases in *A3* expression, such as for *A3A*, can be attributed readily to a few contaminating $CD14^+$ cells in the T lymphocyte preparations. Rather, the strong IFN responsiveness of the *A3*s, highlighted by *A3A*, may be a property of other blood cell lineages such as $CD14^+$ monocytes and macrophages (11,35,39). We also found that T-cell activation with IL-2 and PHA causes the induction of 6/7 *A3*s [i.e. all but A3A; Figure 4B and refs. (35,36)]. These studies combine to indicate that cells have multiple mechanisms to regulate *A3* expression. Thus, in addition to constitutive expression of most of the *A3* repertoire in many cell types and tissues, transcriptional regulation is likely to have a major role in ultimately determining the efficacy and potency of A3-dependent defenses against viral and non-viral challenges.

Overall, turning back to the question of HIV-1 restriction, our studies are consistent with A3F, A3G and potentially several other A3s being important in $CD4^+$ T lymphocytes. A3H is the most likely additional restriction factor because (i) it is expressed in the non-permissive T-cell line H9 (Figure 2), (ii) it is expressed in naïve $CD4^+$ cells (Figure 3), (iii) it is induced 20-fold by T-cell activation (Figure 3), and (iv) it is capable of HIV-1 restriction in a Vif-susceptible manner (20,51–55). Although the literature overwhelmingly favors a role for A3G in HIV-1 restriction, with A3F a distant but important second, A3H and several of the other A3s warrant substantive additional investigation.

SUPPLEMENTARY DATA

Supplementary Data are available at NAR Online.

ACKNOWLEDGEMENTS

The authors thank J. Hultquist for comments on the manuscript, M. Malim for provocative discussion at Cold Spring Harbor, the AIDS Research and Reference Reagent Program for cell lines and antibodies, and D. Bernlohr for the use of a BioRad icycler.

FUNDING

National Institutes of Health (grants GM090437 and AI064046); Bill and Melinda Gates Foundation; Children's Cancer Research Fund (Minneapolis, MN) 3M Graduate Fellowship and a Cancer Biology Training Grant (CA009138) to M.D.S. Funding for open access charge: National Institutes of Health.

Conflict of interest statement. None declared.

REFERENCES

1. Chiu,Y.L. and Greene,W.C. (2008) The APOBEC3 cytidine deaminases: an innate defensive network opposing exogenous retroviruses and endogenous retroelements. *Annu. Rev. Immunol.*, **26**, 317–353.
2. Goila-Gaur,R. and Strebel,K. (2008) HIV-1 Vif, APOBEC, and intrinsic immunity. *Retrovirology*, **5**, 51.
3. Hultquist,J.F. and Harris,R.S. (2009) Leveraging APOBEC3 proteins to alter the HIV mutation rate and combat AIDS. *Future Virol.*, **4**, 605–619.
4. Malim,M.H. and Emerman,M. (2008) HIV-1 accessory proteins–ensuring viral survival in a hostile environment. *Cell Host Microbe*, **3**, 388–398.
5. Sheehy,A.M., Gaddis,N.C., Choi,J.D. and Malim,M.H. (2002) Isolation of a human gene that inhibits HIV-1 infection and is suppressed by the viral Vif protein. *Nature*, **418**, 646–650.
6. Mangeat,B., Turelli,P., Caron,G., Friedli,M., Perrin,L. and Trono,D. (2003) Broad antiretroviral defence by human APOBEC3G through lethal editing of nascent reverse transcripts. *Nature*, **424**, 99–103.
7. Zhang,H., Yang,B., Pomerantz,R.J., Zhang,C., Arunachalam,S.C. and Gao,L. (2003) The cytidine deaminase CEM15 induces hypermutation in newly synthesized HIV-1 DNA. *Nature*, **424**, 94–98.
8. Derse,D., Hill,S.A., Princler,G., Lloyd,P. and Heidecker,G. (2007) Resistance of human T cell leukemia virus type 1 to APOBEC3G restriction is mediated by elements in nucleocapsid. *Proc. Natl Acad. Sci. USA*, **104**, 2915–2920.
9. Lee,Y.N., Malim,M.H. and Bieniasz,P.D. (2008) Hypermutation of an ancient human retrovirus by APOBEC3G. *J. Virol.*, **82**, 8762–8770.
10. Suspène,R., Guétard,D., Henry,M., Sommer,P., Wain-Hobson,S. and Vartanian,J.P. (2005) Extensive editing of both hepatitis B virus DNA strands by APOBEC3 cytidine deaminases in vitro and in vivo. *Proc. Natl Acad. Sci. USA*, **102**, 8321–8326.

11. Stenglein,M.D., Burns,M.B., Li,M., Lengyel,J. and Harris,R.S. (2010) APOBEC3 proteins mediate the clearance of foreign DNA from human cells. *Nat. Struct. Mol. Biol.*, **17**, 222–229.
12. Vartanian,J.P., Guetard,D., Henry,M. and Wain-Hobson,S. (2008) Evidence for editing of human papillomavirus DNA by APOBEC3 in benign and precancerous lesions. *Science*, **320**, 230–233.
13. Bogerd,H.P., Wiegand,H.L., Hulme,A.E., Garcia-Perez,J.L., O'Shea,K.S., Moran,J.V. and Cullen,B.R. (2006) Cellular inhibitors of long interspersed element 1 and Alu retrotransposition. *Proc. Natl Acad. Sci. USA*, **103**, 8780–8785.
14. Chiu,Y.L., Witkowska,H.E., Hall,S.C., Santiago,M., Soros,V.B., Esnault,C., Heidmann,T. and Greene,W.C. (2006) High-molecular-mass APOBEC3G complexes restrict Alu retrotransposition. *Proc. Natl Acad. Sci. USA*, **103**, 15588–15593.
15. Muckenfuss,H., Hamdorf,M., Held,U., Perkovic,M., Lower,J., Cichutek,K., Flory,E., Schumann,G.G. and Munk,C. (2006) APOBEC3 proteins inhibit human LINE-1 retrotransposition. *J. Biol. Chem.*, **281**, 22161–22172.
16. Albin,J.S. and Harris,R.S. (2010) Interactions of host APOBEC3 restriction factors with HIV-1 in vivo: implications for therapeutics. *Expert Rev. Mol. Med.*, **12**, e4.
17. Jarmuz,A., Chester,A., Bayliss,J., Gisbourne,J., Dunham,I., Scott,J. and Navaratnam,N. (2002) An anthropoid-specific locus of orphan C to U RNA-editing enzymes on chromosome 22. *Genomics*, **79**, 285–296.
18. LaRue,R.S., Jónsson,S.R., Silverstein,K.A.T., Lajoie,M., Bertrand,D., El-Mabrouk,N., Hötzel,I., Andrésdóttir,V., Smith,T.P.L. and Harris,R.S. (2008) The artiodactyl APOBEC3 innate immune repertoire shows evidence for a multi-functional domain organization that existed in the ancestor of placental mammals. *BMC Mol. Biol.*, **9**, 104.
19. Kidd,J.M., Newman,T.L., Tuzun,E., Kaul,R. and Eichler,E.E. (2007) Population stratification of a common APOBEC gene deletion polymorphism. *PLoS Genet.*, **3**, e63.
20. OhAinle,M., Kerns,J.A., Li,M.M., Malik,H.S. and Emerman,M. (2008) Antiretroelement activity of APOBEC3H was lost twice in recent human evolution. *Cell Host Microbe*, **4**, 249–259.
21. Sawyer,S.L., Emerman,M. and Malik,H.S. (2004) Ancient adaptive evolution of the primate antiviral DNA-editing enzyme APOBEC3G. *PLoS Biol.*, **2**, E275.
22. Haché,G., Shindo,K., Albin,J.S. and Harris,R.S. (2008) Evolution of HIV-1 isolates that use a novel Vif-independent mechanism to resist restriction by human APOBEC3G. *Curr. Biol.*, **18**, 819–824.
23. Pfaffl,M.W. (2001) A new mathematical model for relative quantification in real-time RT-PCR. *Nucleic Acids Res.*, **29**, e45.
24. Peirson,S.N., Butler,J.N. and Foster,R.G. (2003) Experimental validation of novel and conventional approaches to quantitative real-time PCR data analysis. *Nucleic Acids Res.*, **31**, e73.
25. Holmes,R.K., Koning,F.A., Bishop,K.N. and Malim,M.H. (2007) APOBEC3F can inhibit the accumulation of HIV-1 reverse transcription products in the absence of hypermutation. Comparisons with APOBEC3G. *J. Biol. Chem.*, **282**, 2587–2595.
26. Newman,E.N., Holmes,R.K., Craig,H.M., Klein,K.C., Lingappa,J.R., Malim,M.H. and Sheehy,A.M. (2005) Antiviral function of APOBEC3G can be dissociated from cytidine deaminase activity. *Curr. Biol.*, **15**, 166–170.
27. Harris,R.S., Petersen-Mahrt,S.K. and Neuberger,M.S. (2002) RNA editing enzyme APOBEC1 and some of its homologs can act as DNA mutators. *Mol. Cell*, **10**, 1247–1253.
28. Gabuzda,D.H., Lawrence,K., Langhoff,E., Terwilliger,E., Dorfman,T., Haseltine,W.A. and Sodroski,J. (1992) Role of Vif in replication of human immunodeficiency virus type 1 in CD4+ T lymphocytes. *J. Virol.*, **66**, 6489–6495.
29. Strebel,K., Daugherty,D., Clouse,K., Cohen,D., Folks,T. and Martin,M.A. (1987) The HIV 'A' (sor) gene product is essential for virus infectivity. *Nature*, **328**, 728–730.
30. von Schwedler,U., Song,J., Aiken,C. and Trono,D. (1993) Vif is crucial for human immunodeficiency virus type 1 proviral DNA synthesis in infected cells. *J. Virol.*, **67**, 4945–4955.
31. Bishop,K.N., Holmes,R.K., Sheehy,A.M., Davidson,N.O., Cho,S.J. and Malim,M.H. (2004) Cytidine deamination of retroviral DNA by diverse APOBEC proteins. *Curr. Biol.*, **14**, 1392–1396.
32. Yu,Q., Chen,D., Konig,R., Mariani,R., Unutmaz,D. and Landau,N.R. (2004) APOBEC3B and APOBEC3C are potent inhibitors of simian immunodeficiency virus replication. *J. Biol. Chem.*, **279**, 53379–53386.
33. Chen,H., Lilley,C.E., Yu,Q., Lee,D.V., Chou,J., Narvaiza,I., Landau,N.R. and Weitzman,M.D. (2006) APOBEC3A is a potent inhibitor of adeno-associated virus and retrotransposons. *Curr. Biol.*, **16**, 480–485.
34. Peng,G., Greenwell-Wild,T., Nares,S., Jin,W., Lei,K.J., Rangel,Z.G., Munson,P.J. and Wahl,S.M. (2007) Myeloid differentiation and susceptibility to HIV-1 are linked to APOBEC3 expression. *Blood*, **110**, 393–400.
35. Koning,F.A., Newman,E.N., Kim,E.Y., Kunstman,K.J., Wolinsky,S.M. and Malim,M.H. (2009) Defining APOBEC3 expression patterns in human tissues and hematopoietic cell subsets. *J. Virol.*, **83**, 9474–9485.
36. Stopak,K.S., Chiu,Y.L., Kropp,J., Grant,R.M. and Greene,W.C. (2007) Distinct patterns of cytokine regulation of APOBEC3G expression and activity in primary lymphocytes, macrophages, and dendritic cells. *J. Biol. Chem.*, **282**, 3539–3546.
37. Argyris,E.G., Acheampong,E., Wang,F., Huang,J., Chen,K., Mukhtar,M. and Zhang,H. (2007) The interferon-induced expression of APOBEC3G in human blood-brain barrier exerts a potent intrinsic immunity to block HIV-1 entry to central nervous system. *Virology*, **367**, 440–451.
38. Bonvin,M., Achermann,F., Greeve,I., Stroka,D., Keogh,A., Inderbitzin,D., Candinas,D., Sommer,P., Wain-Hobson,S., Vartanian,J.P. *et al.* (2006) Interferon-inducible expression of APOBEC3 editing enzymes in human hepatocytes and inhibition of hepatitis B virus replication. *Hepatology*, **43**, 1364–1374.
39. Chen,K., Huang,J., Zhang,C., Huang,S., Nunnari,G., Wang,F.X., Tong,X., Gao,L., Nikisher,K. and Zhang,H. (2006) Alpha interferon potently enhances the anti-human immunodeficiency virus type 1 activity of APOBEC3G in resting primary CD4 T cells. *J. Virol.*, **80**, 7645–7657.
40. Peng,G., Lei,K.J., Jin,W., Greenwell-Wild,T. and Wahl,S.M. (2006) Induction of APOBEC3 family proteins, a defensive maneuver underlying interferon-induced anti-HIV-1 activity. *J. Exp. Med.*, **203**, 41–46.
41. Tanaka,Y., Marusawa,H., Seno,H., Matsumoto,Y., Ueda,Y., Kodama,Y., Endo,Y., Yamauchi,J., Matsumoto,T., Takaori-Kondo,A. *et al.* (2006) Anti-viral protein APOBEC3G is induced by interferon-alpha stimulation in human hepatocytes. *Biochem. Biophys. Res. Commun.*, **341**, 314–319.
42. Wang,F.X., Huang,J., Zhang,H., Ma,X. and Zhang,H. (2008) APOBEC3G upregulation by alpha interferon restricts human immunodeficiency virus type 1 infection in human peripheral plasmacytoid dendritic cells. *J. Gen. Virol.*, **89**, 722–730.
43. Vetter,M.L., Johnson,M.E., Antons,A.K., Unutmaz,D. and D'Aquila,R.T. (2009) Differences in APOBEC3G expression in CD4+ T helper lymphocyte subtypes modulate HIV-1 infectivity. *PLoS Pathog.*, **5**, e1000292.
44. Taylor,M.W., Grosse,W.M., Schaley,J.E., Sanda,C., Wu,X., Chien,S.C., Smith,F., Wu,T.G., Stephens,M., Ferris,M.W. *et al.* (2004) Global effect of PEG-IFN-alpha and ribavirin on gene expression in PBMC in vitro. *J. Interferon Cytokine Res.*, **24**, 107–118.
45. Swirski,F.K., Nahrendorf,M., Etzrodt,M., Wildgruber,M., Cortez-Retamozo,V., Panizzi,P., Figueiredo,J.L., Kohler,R.H., Chudnovskiy,A., Waterman,P. *et al.* (2009) Identification of splenic reservoir monocytes and their deployment to inflammatory sites. *Science*, **325**, 612–616.
46. Daniele,R.P., Dauber,J.H., Altose,M.D., Rowlands,D.T. Jr and Gorenberg,D.J. (1977) Lymphocyte studies in asymptomatic cigarette smokers. A comparison between lung and peripheral blood. *Am. Rev. Respir. Dis.*, **116**, 997–1005.
47. Weisberg,S.P., McCann,D., Desai,M., Rosenbaum,M., Leibel,R.L. and Ferrante,A.W. Jr (2003) Obesity is associated with macrophage accumulation in adipose tissue. *J. Clin. Invest.*, **112**, 1796–1808.
48. Stenglein,M.D. and Harris,R.S. (2006) APOBEC3B and APOBEC3F inhibit L1 retrotransposition by a DNA deamination-independent mechanism. *J. Biol. Chem.*, **281**, 16837–16841.

49. Haché,G. and Harris,R.S. (2009) CEM-T4 cells do not lack an APOBEC3G cofactor. *PLoS Pathog.*, **5**, e1000528.
50. Esnault,C., Heidmann,O., Delebecque,F., Dewannieux,M., Ribet,D., Hance,A.J., Heidmann,T. and Schwartz,O. (2005) APOBEC3G cytidine deaminase inhibits retrotransposition of endogenous retroviruses. *Nature*, **433**, 430–433.
51. Dang,Y., Siew,L.M., Wang,X., Han,Y., Lampen,R. and Zheng,Y.H. (2008) Human cytidine deaminase APOBEC3H restricts HIV-1 replication. *J. Biol. Chem.*, **283**, 11606–11614.
52. Harari,A., Ooms,M., Mulder,L.C. and Simon,V. (2009) Polymorphisms and splice variants influence the antiretroviral activity of human APOBEC3H. *J. Virol.*, **83**, 295–303.
53. OhAinle,M., Kerns,J.A., Malik,H.S. and Emerman,M. (2006) Adaptive evolution and antiviral activity of the conserved mammalian cytidine deaminase APOBEC3H. *J. Virol.*, **80**, 3853–3862.
54. Tan,L., Sarkis,P.T., Wang,T., Tian,C. and Yu,X.F. (2009) Sole copy of Z2-type human cytidine deaminase APOBEC3H has inhibitory activity against retrotransposons and HIV-1. *FASEB J.*, **23**, 279–287.
55. Li,M.M., Wu,L.I. and Emerman,M. (2010) The range of human APOBEC3H sensitivity to lentiviral Vif proteins. *J. Virol.*, **84**, 88–95.
56. Liddament,M.T., Brown,W.L., Schumacher,A.J. and Harris,R.S. (2004) APOBEC3F properties and hypermutation preferences indicate activity against HIV-1 *in vivo*. *Curr. Biol.*, **14**, 1385–1391.
57. Henry,M., Guetard,D., Suspene,R., Rusniok,C., Wain-Hobson,S. and Vartanian,J.P. (2009) Genetic editing of HBV DNA by monodomain human APOBEC3 cytidine deaminases and the recombinant nature of APOBEC3G. *PloS ONE*, **4**, e4277.
58. Kock,J. and Blum,H.E. (2008) Hypermutation of hepatitis B virus genomes by APOBEC3G, APOBEC3C and APOBEC3H. *J. Gen. Virol.*, **89**, 1184–1191.
59. Jost,S., Turelli,P., Mangeat,B., Protzer,U. and Trono,D. (2007) Induction of antiviral cytidine deaminases does not explain the inhibition of hepatitis B virus replication by interferons. *J. Virol.*, **81**, 10588–10596.
60. Narvaiza,I., Linfesty,D.C., Greener,B.N., Hakata,Y., Pintel,D.J., Logue,E., Landau,N.R. and Weitzman,M.D. (2009) Deaminase-independent inhibition of parvoviruses by the APOBEC3A cytidine deaminase. *PLoS Pathog.*, **5**, e1000439.